

Multifocal ERG in subjects with a history of retinopathy of prematurity

Anne B. Fulton, Ronald M. Hansen, Anne Moskowitz & Amber M. Barnaby
Department of Ophthalmology, Children's Hospital and Harvard Medical School, Boston, MA, USA

Accepted 19 August 2005

Key words: multifocal ERG, retinopathy of prematurity

Abstract

Purpose: Investigate the function of the central retina in subjects with a history of retinopathy of prematurity (ROP). *Methods:* Multifocal electroretinogram (mfERG) responses to a scaled array of 103 hexagons were recorded in subjects, aged 11–23 years ($N=11$), with a documented history of mild ROP. The amplitude and implicit time of the components (N_1 , P_1 , N_2) of the first order kernel for six concentric rings were compared to those of control subjects ($N=9$). *Results:* The amplitude of each component varied significantly with eccentricity in both ROP and control subjects and was significantly smaller in the ROP subjects. The discrepancy between ROP and control subjects was greatest for central rings (1–3) and smaller for peripheral rings (4–6). The slopes of the functions summarizing log response density as a function of log eccentricity (degrees visual angle) were significantly shallower in ROP subjects. The implicit time of each component was longer in ROP subjects at all eccentricities. *Conclusions:* ROP associated alterations in neural retinal development may underlie the subtle macular dysfunction disclosed by the mfERG.

Introduction

The development of the central retina, the region in which the photoreceptors mature last [1–3], is altered by retinopathy of prematurity (ROP). Subjects with a history of mild ROP have a slower than normal course of development of the rod mediated visual threshold in the parafoveal retina, 10° eccentric from the fovea, and in some subjects, mild elevation of these thresholds persists into adolescence and early adulthood [4–6].

ROP also alters the development of the fovea, which forms in a rod free zone at the very center of the macula. In normal foveal development, the diameter of the rod free zone decreases from approximately $1400\ \mu\text{m}$ at 26 weeks gestation to $500\ \mu\text{m}$ in the mature eye as cone outer segments elongate and inner segments become more slender [7–10]. The foveal cone outer segments pack more tightly together, affording improved acuity [7, 9–12]. The foveal cone nuclei and inner retinal cells move away from the tightly packed foveal

cone outer segments [13]. Thus, as normal development proceeds, the distance from the center of the fovea to the cone photoreceptor nuclei and bipolar cells increases [13]. As at other sites in the nervous system [14], there is an interaction between the developing neural cells and the retinal vasculature [10, 15]. A ring of parafoveal vasculature defines the developing foveal dimple [13, 15] and the mature foveal avascular zone which subtends $\sim 2^\circ$ visual angle.

At term (40 weeks gestation), the foveal dimple is normally identifiable by ophthalmoscopy. In preterm infants, the formation of the foveal dimple is delayed in those with ROP even if all clinically visible ROP is peripheral to the macula [16]. Furthermore, in former preterms with no ROP involvement of the macula, the foveal avascular zone, as determined by fluorescein angiography in childhood, has a smaller diameter than in term born children [17]. It is not uncommon for children and adolescents with a history of mild ROP to have mild deficits in letter acuity

that cannot be corrected by careful refraction, even in the absence of clinical ROP in the macula and the absence of early high refractive errors [6]. Thus, measures of visual function mediated by the central retina [5, 6] and observations of macular structure [16, 17] suggest that ROP alters the development of the central retina. However, function of the central retinal cells has not yet been studied directly. We used the multifocal electroretinogram (mfERG) to test the photopic function of the central retina in older children and young adults with a history of mild ROP.

Subjects and methods

Subjects

Eleven ROP subjects (Table 1), each of whom had been followed in this department since infancy, were age 11–23 (median 13) years at the time of the mfERG test. All had a documented history of mild ROP that resolved spontaneously leaving no ophthalmoscopically visible residua. On clinical examination, each was judged to have a normal macula with an identifiable foveal dimple. Over their first 4 years, none had spherical equivalents outside the 99% prediction interval for normal [18, 19]; seven had become myopic by the time of the mfERG test (Table 1). The median spherical equivalent was -3.00 (range -6.88 to $+0.37$) diopters. ETDRS acuity (Table 1),

with correction if indicated, ranged from -0.1 to 0.26 logMAR (20/16–20/36). The spherical equivalent and visual acuity of the right eye of each subject was similar to that shown for the left eye (Table 1) with the exception of Subject 1 whose right eye had high myopia, low acuity and dragged macula.

Nine control subjects, age 23–51 (median 25) years, with corrected letter acuities of -0.12 to 0.08 logMAR (20/15–20/24) were also tested. The range of spherical equivalents (-7.50 diopters to Plano; median -0.88 diopters) in the control subjects overlapped that in the ROP subjects.

Written, informed consent was obtained from all subjects older than 18 years and from the parents of the children. The study conformed to the Tenets of the Declaration of Helsinki and was approved by the Children’s Hospital Committee on Clinical Investigation.

mfERG procedure

The left pupil was dilated with cyclopentolate hydrochloride 1% and phenylephrine hydrochloride 2.5%. Following instillation of proparacaine 0.5%, a Burian Allen bipolar electrode was placed on the left eye, and a ground electrode was placed on the skin over the left mastoid. The mfERG responses were obtained using the VERIS software (EDI, San Mateo, CA) and a scaled array of 103 hexagons. The stimulus display subtended 20° to each side of a central fixation cross, with the central hexagon subtending approximately 2° .

Table 1. Characteristics of ROP subjects

Subject #	Birth weight (grams)	Gestational age at birth (weeks)	Age (years)	Spherical equivalent left eye (diopters)	Visual acuity left eye	
					logMAR	Snellen
1	780	26.0	11	-4.25	-0.10	20/16
2	800	26.0	12	$+0.37$	0.02	20/21
3	600	24.0	13	Plano	-0.05	20/18
4	730	24.0	13	Plano	0.20	20/32
5	820	26.0	13	-4.00	0.06	20/23
6	860	26.0	13	-2.50	0.26	20/36
7	1050	27.0	19	-6.88	-0.07	20/17
8	1077	25.0	22	-3.00	0.02	20/21
9	1700	29.5	22	Plano	0.24	20/35
10	790	27.0	22	-4.75	0.02	20/21
11	790	27.5	23	-3.00	0.00	20/20
Median	800	26.0	13	-3.00	0.02	20/21

The stimulus luminance was 100 cd/m^2 . Each element changed from dark to light ($\sim 95\%$ contrast) repeatedly and randomly under control of an m-sequence [20]. Subjects wore refractive correction during the mfERG test.

The amplitude (nV/deg^2) and implicit time (ms) of the three components (N_1 , P_1 , N_2) of the first order kernel were evaluated as a function of eccentricity (ring 1, 2, 3, 4, 5 and 6). Amplitude was measured from the baseline to the trough (N_1 , N_2) or peak (P_1) of the deflection. Implicit time was measured from the start of the trace to the trough or peak.

Additionally, amplitude of the P_1 response in individual hexagons along the horizontal meridian was plotted as a function of nasal and temporal eccentricity (degrees visual angle) on log-log coordinates [21]; the response to the central hexagon, centered at zero degrees, was excluded from this analysis. The slopes of the resulting functions for ROP and control subjects were compared.

Results

Sample records of the responses to the 103 hexagons are shown for an ROP and a control subject in Figure 1. Ring averages are compared in Figure 2.

The mean amplitudes of N_1 , P_1 and N_2 (Figure 3) are significantly smaller in the ROP subjects, and each component varies significantly with eccentricity (Table 2). Results of two factor (Group: ROP, Control; Eccentricity: Ring number 1,2,3,4,5,6) analysis of variance are summarized in Table 2. The difference is greatest for the central rings, less for the peripheral rings.

Implicit times of N_1 , P_1 , and N_2 (Figure 4) are consistently longer in ROP subjects at all eccentricities. For N_1 and P_1 , implicit time changes little with eccentricity. For N_2 , implicit time decreases slightly with eccentricity in both groups of subjects.

When amplitude (nV/deg^2) is examined as a function of eccentricity expressed in physical units, degrees visual angle, the difference between ROP and control subjects is further characterized as shown in the log-log plots (Figure 5, upper panel). In the lower panel, the nasal and temporal slopes of the log-log functions for each subject are summarized. The mean slopes of the ROP subjects in both nasal (-0.32 , $\text{SD}=0.134$) and temporal (-0.23 , $\text{SD}=0.093$) fields are lower than in the controls (nasal: -0.79 , $\text{SD}=0.277$; temporal: -0.61 , $\text{SD}=0.27$). These differences are significant in both nasal ($t=4.96$; $\text{df}=18$; $p<0.01$) and temporal ($t=4.38$; $\text{df}=18$; $p<0.01$) fields. Within individual subjects, the slopes in the nasal field (temporal retina) are significantly

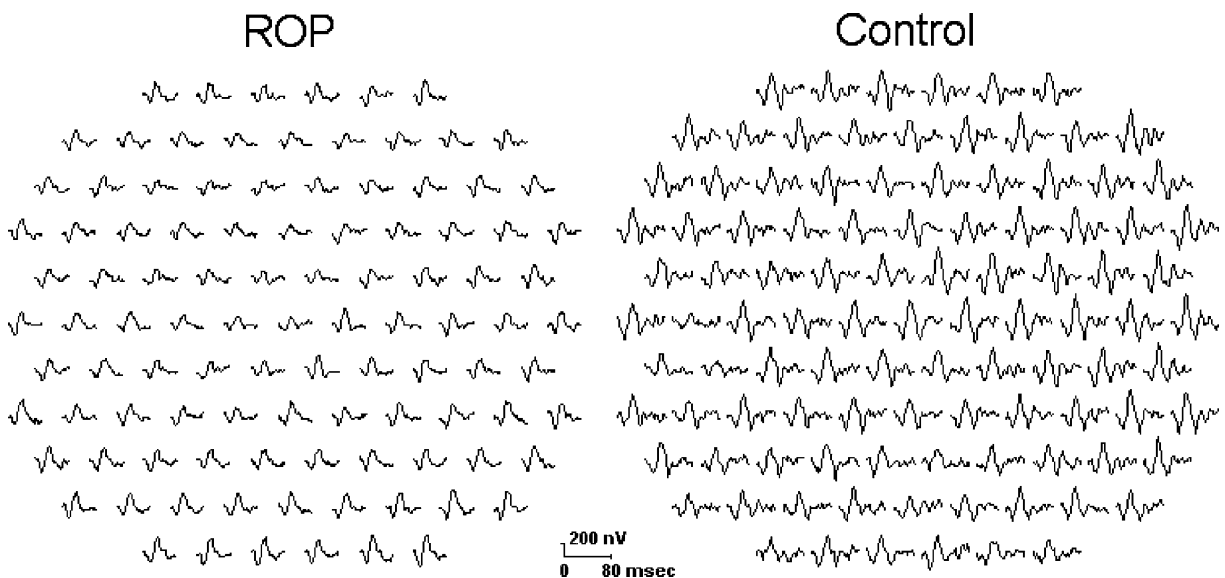


Figure 1. Sample record. 103 responses from ROP subject 3 (Table 1) and a 22-year-old control subject with -2.75 diopter spherical equivalent.

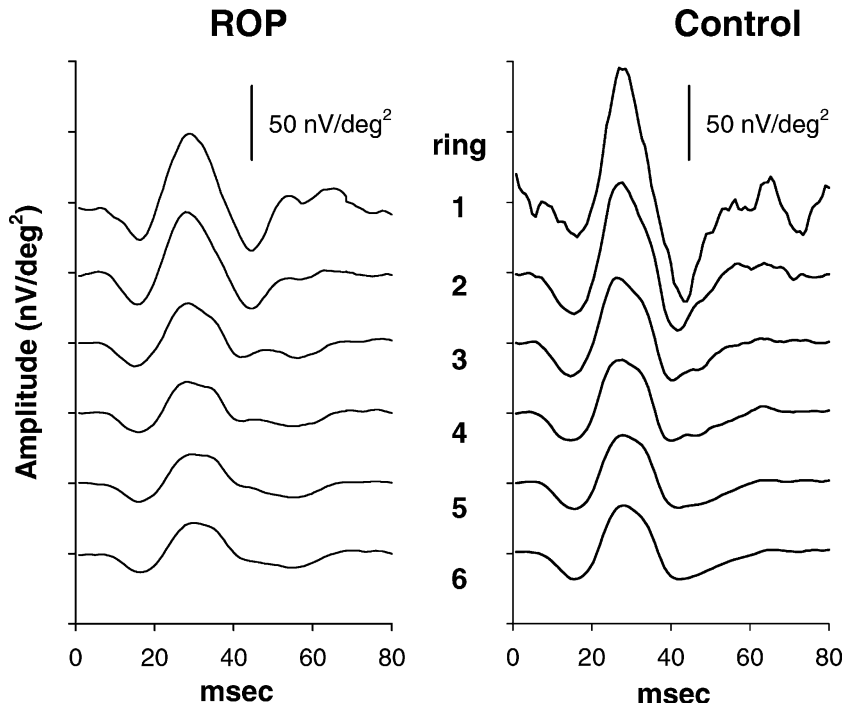


Figure 2. Comparison of responses from ROP subject 2 (Table 1) and a 50-year-old control subject with Plano spherical equivalent. The responses to the central hexagon (ring 1) and the average of responses to all hexagons in each concentric ring (2–6) are shown. In the ROP subject, the amplitudes are smaller and the implicit times longer.

steeper than in the temporal field (nasal retina) ($t = 4.6$; $df = 19$; $p < 0.01$).

Neither letter acuity nor spherical equivalent is related to the amplitude or the implicit time of any component (N_1 , P_1 , N_2) at any eccentricity. There are no significant correlations of nasal or temporal slope with visual acuity or spherical equivalent for either ROP or control subjects.

Discussion

Among these subjects whose clinical ROP had resolved completely more than a decade or two earlier, significant deficits in amplitude and implicit time of mfERG responses are found. It seems unlikely that the difference in age between the ROP and control groups explain these deficits because with normal aging, amplitude decreases (about 3–7% per decade) and implicit time increases (about 0.7–2.2% per decade) [22–24]. It is our younger group, the ROP group, that had lower amplitudes and longer implicit times.

The most marked difference in amplitude density between ROP and control subjects is in rings

1, 2 and 3 (Figure 2) that subtend a total horizontal distance of $\sim 6^\circ$ visual angle in the mature eye. Interestingly, at 26 weeks gestation, the median gestational age at birth for our ROP subjects (Table 1), the diameter of the rod free zone is $1400 \mu\text{m}$ [7–10]. The dimension $1400 \mu\text{m}$ in the small, 26 week gestational age eye with axial length $\sim 12.5 \text{ mm}$ [25–27] and posterior nodal distance $\sim 2/3$ the axial length [28], subtends approximately 6.5° visual angle. This provocative coincidence suggests that ROP alters the development of the central retina. We suspect that the developmental re-distribution of the central-most retinal cells is altered in ROP subjects. The large discrepancy between the ROP and control amplitude in the central-most rings raises the possibility that the difference in bipolar cell density between ROP and control subjects is greatest in the central-most retina. Bipolar cells make main contributions to the mfERG components that we have studied [29].

The lower amplitudes do not necessarily mean that there are fewer bipolar cells per unit area in the most central retina of ROP subjects. If ROP associated effects on foveal development [16, 30]

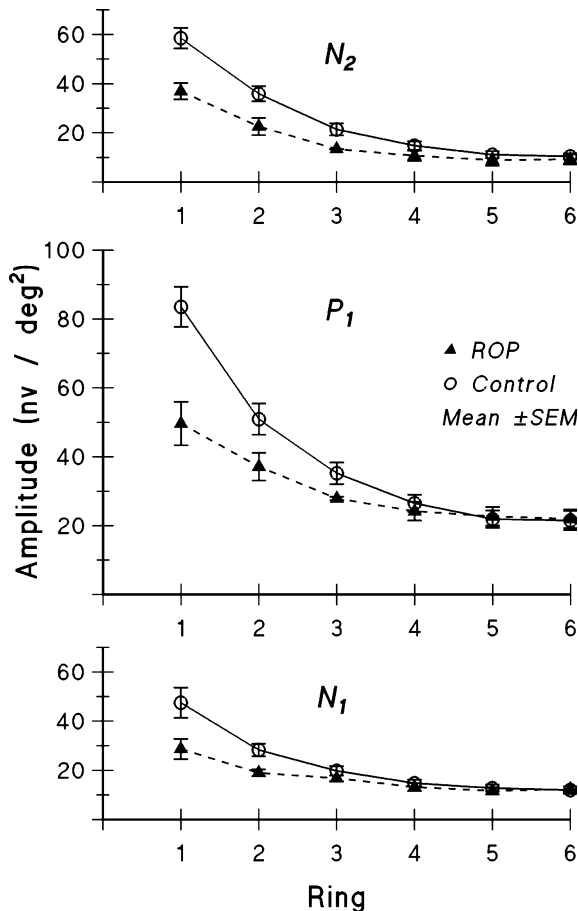


Figure 3. Mean amplitudes (\pm SE) for ROP and control subjects for each component, N_1 , P_1 , and N_2 , of the first order kernel are plotted for each ring, 1 through 6. The difference between ROP and control subjects is greatest for the central-most rings.

impair the normal centrifugal movement of foveal cone nuclei and inner retinal cells [13, 31], a higher than normal density of bipolar cells would be forecast in the central-most ROP retina, a

Table 2. Results of analysis of variance for amplitude

Component	Factor	F	df	<i>p</i>
N1	ROP/CTL	13.29	1,6	<0.01
	Eccentricity	26.93	5,6	<0.01
P1	ROP/CTL	15.52	1,6	<0.01
	Eccentricity	33.77	5,6	<0.01
N2	ROP/CTL	18.39	1,6	<0.01
	Eccentricity	36.84	5,6	<0.01

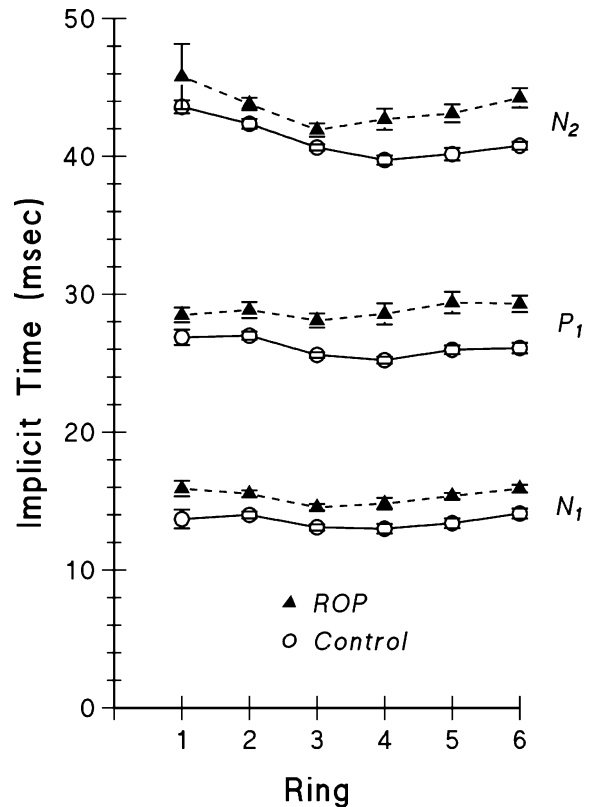


Figure 4. Mean (\pm SE) implicit time for the ROP and control subjects for each component, N_1 , P_1 , and N_2 , of the first order kernel are plotted for each ring, 1 through 6. The implicit times differ between ROP and control subjects at all eccentricities.

prediction that could be tested using ultrahigh-resolution coherence tomography [32]. Because the activity of both ON and OFF bipolar cells contribute to the P_1 component of the mfERG [29], possibly the summation of hyperpolarizing and depolarizing activity in ROP subjects is such that amplitudes are smaller, especially in the central-most retina. At the same time, the difference between ROP and control subjects' implicit time is nearly constant across all eccentricities. Therefore, it would not be surprising to find the summing of ON and OFF bipolar activity to be altered throughout the ROP retina. Further information on this matter can be obtained by studying the cone mediated ERG response to full field stimuli. Study of the development of mfERG responses in infants with a history of ROP [33], as well as study of adolescent subjects using other modalities such as psychophysical

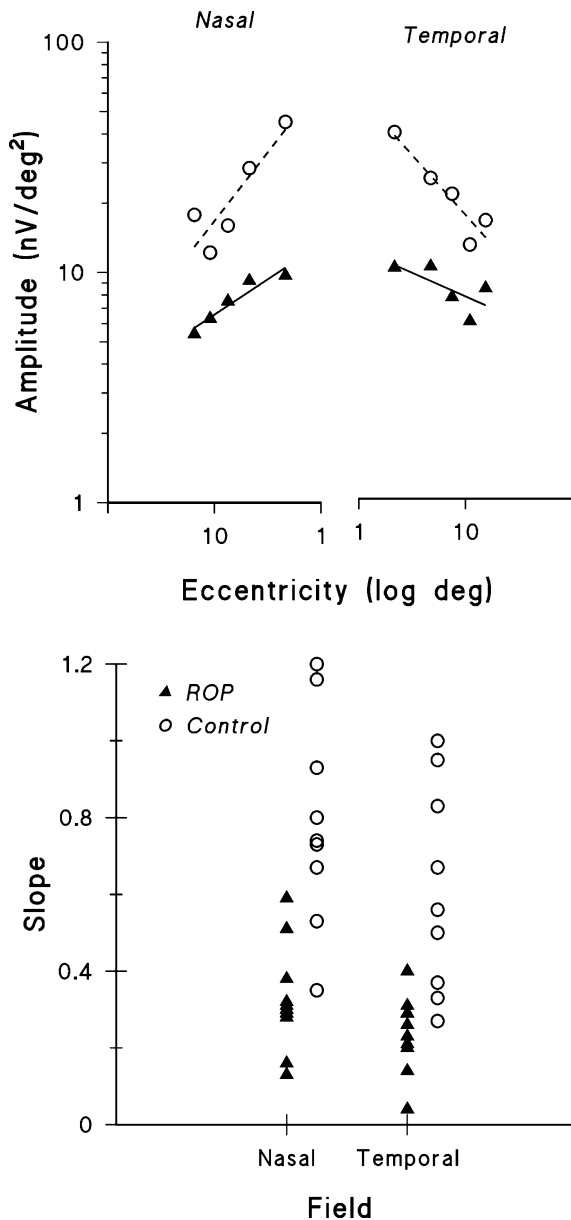


Figure 5. Upper panel: Sample log–log plots of amplitude as a function of eccentricity in degrees visual angle. The data are from ROP subject 6 (\blacktriangle) and a 50 year control subject with Plano spherical equivalent (\circ). The slopes of the regression lines fit to their data are near the median values for the ROP and control groups. Lower panel: Slopes for every subject in nasal and temporal field. The slopes in the ROP subjects are significantly lower than in the control subjects.

procedures for assessment of directional sensitivity (Stiles-Crawford effects) and adaptive optics [34–36], can be expected to further our understanding of the effects of ROP on the central retina, including the fovea and parafoveal cones.

Acknowledgements

This study was supported in part by NIH grant EY 10597. We thank Baharek Asefzadah and Annie Gee for their assistance.

References

1. Grun G. The development of the vertebrate retina: a comparative survey. *Adv Anat Embryol Cell Biol* 1982; 78: 1–85.
2. Dorn EM, Hendrickson L, Hendrickson AE. The appearance of rod opsin during monkey retinal development. *Invest Ophthalmol Vis Sci* 1995; 36(13): 2634–51.
3. Drucker D, Hendrickson AE. The morphological development of extrafoveal human retina. *Invest Ophthalmol Vis Sci* 1989; 30(suppl): 226.
4. Fulton AB, Hansen RM. Rod photoreceptor function in ROP. *Mol Vision* 2005 (in press).
5. Jolesz M, Vanderveen DK, Hansen RM, Fulton A. Development of rod mediated visual thresholds in infants with a history of mild retinopathy of prematurity. *Invest Ophthalmol Vis Sci* 2002; ARVO Abstract 2864.
6. Reiser DS, Hansen RM, Findl O, Petersen RA, Fulton AB. Dark-adapted thresholds in children with histories of mild retinopathy of prematurity. *Invest Ophthalmol Vis Sci* 1997; 38(6): 1175–83.
7. Yuodelis C, Hendrickson A. A qualitative and quantitative analysis of the human fovea during development. *Vision Res* 1986; 26(6): 847–55.
8. Hendrickson A, Yuodelis C. The morphological development of the human fovea. *Ophthalmology* 1984; 91: 603–12.
9. Hendrickson AE. The morphologic development of human and monkey retina. *Principles and Practice of Ophthalmology: Basic Sciences*. In: Albert DM, Jakobiec FA, eds. *Principles and Practice of Ophthalmology: Basic Sciences*, Philadelphia: WB Saunders Co., 1994: 561–77.
10. Hendrickson AE. Primate foveal development: a microcosm of current questions in neurobiology. *Invest Ophthalmol Vis Sci* 1994; 35: 3129–33.
11. Springer AD, Hendrickson AE. Development of the primate area of high acuity. 1. Use of finite element analysis models to identify mechanical variables affecting pit formation. *Visual Neurosci* 2004; 21(1): 53–62.
12. Blakemore C. Maturation of mechanisms for efficient spatial vision. *Vision: Coding and Efficiency*. In: Blakemore C, eds. *Vision: Coding and Efficiency*, Cambridge: Cambridge University Press, 1990: 256–66.
13. Springer AD. New role for the primate fovea: a retinal excavation determines photoreceptor deployment and shape. *Vis Neurosci* 1999; 16(4): 629–36.
14. Soker S, Takashima S, Miao HQ, Neufeld G, Klagsbrun M. Neuropilin-1 is expressed by endothelial and tumor cells as an isoform-specific receptor for vascular endothelial growth factor. *Cell* 1998; 92: 735–42.
15. Provis JM, Sandercoe T, Hendrickson AE. Astrocytes and blood vessels define the foveal rim during primate retinal development. *Invest Ophthalmol Vis Sci* 2000; 41(10): 2827–36.
16. Isenberg SJ. Macular development in the premature infant. *Am J Ophthalmol* 1986; 101: 74–80.

17. Mintz-Hittner HA, Knight-Nanan DM, Satriano DR, Kretzer FL. A small foveal avascular zone may be an historic mark of prematurity. *Ophthalmology* 1999; 106: 1409–13.
18. Moskowitz A, Hansen RM, Fulton AB. Early ametropia and rod cell function in retinopathy of prematurity. *Optometry Vision Sci* 2005; 82: 307–317.
19. Mayer DL, Hansen RM, Moore BD, Kim S, Fulton AB. Cycloplegic refractions in healthy children, aged 1 through 48 months. *Arch Ophthalmol* 2001; 119: 1625–28.
20. Sutter EE. Imaging visual function with the multifocal m-sequence technique. *Vision Res* 2001; 41(10–11): 1241–55.
21. Sutter EE, Tran D. The field topography of ERG components in man—I. The photopic luminance response. *Vision Res* 1992; 32(3): 433–46.
22. Tzekov RT, Gerth C, Werner JS. Senescence of human multifocal electroretinogram components: a localized approach. *Graefes Arch Clin Exp Ophthalmol* 2004; 242(7): 549–60.
23. Gerth C, Sutter EE, Werner JS. mfERG response dynamics of the aging retina. *Invest Ophthalmol Vis Sci* 2003; 44(10): 4443–50.
24. Gerth C, Garcia SM, Ma L, Keltner JL, Werner JS. Multifocal electroretinogram: age-related changes for different luminance levels. *Graefes Arch Clin Exp Ophthalmol* 2002; 240(3): 202–8.
25. Robb RM. Increase in retinal surface area during infancy and childhood. *J Ped Ophthalmol Strab* 1982; 19: 16–20.
26. Denis D, Burguiere O, Burillon C. A biometric study of the eye, orbit and face in 205 normal human fetuses. *Invest Ophthalmol Vis Sci* 1998; 39(12): 2232–38.
27. Achiron R, Kreiser D, Achiron A. Axial growth of the fetal eye and evaluation of the hyaloid artery in utero ultrasonographic study. *Prenatal Diagnosis* 2000; 20: 894–9.
28. Troilo D, Howland HC, Judge SJ. Visual optics and retinal cone topography in the common marmoset (*Callithrix jacchus*). *Vision Res* 1993; 33(10): 1301–10.
29. Hood DC, Frishman LJ, Saszik S, Viswanathan S. Retinal origins of the primate multifocal ERG: implications for the human response. *Invest Ophthalmol Vis Sci* 2002; 43(5): 1673–85.
30. Hittner HM, Rhodes LM, McPherson AT. Anterior segment abnormalities in cicatricial retinopathy of prematurity. *Ophthalmol* 1979; 86: 803–16.
31. Ueno S, Kondo M, Yasurhiro N, Terasaki H, Miyake Y. Luminance dependence of neural components that underlies the primate photopic electroretinogram. *Invest Ophthalmol Vis Sci* 2004; 45(3): 1033–40.
32. Ko TH, Fujimoto JG, Duker JS, Paunescu LA, Drexler W, Bauman CR, et al. Comparison of ultrahigh- and standard-resolution optical coherence tomography for imaging macular hole pathology and repair. *Ophthalmology* 2004; 111(11): 2033–43.
33. Hansen RM, Fulton AB. Cone cell function in children with a history of retinopathy of prematurity. *Invest Ophthalmol Vis Sci* 2004; 45: Abstract 1352.
34. Carroll J, Neitz M, Hofer H, Neitz J, Williams DR. Functional photoreceptor loss revealed with adaptive optics: an alternate cause of color blindness. *Proc Natl Acad Sci USA* 2004; 101(22): 8461–6.
35. Liang J, Williams DR, Miller DT. Supernormal vision and high-resolution retinal imaging through adaptive optics. *J Opt Soc Am A Opt Image Sci Vis* 1997; 14(11): 2884–92.
36. Wolfing J, Chung M, Carroll J, Williams DR. High resolution imaging of cone-rod dystrophy (Abstract). *J Vision* 2004; 4(11): 91a.

Address for correspondence: Anne Fulton Children's Hospital Department of Ophthalmology 300 Longwood Avenue, Boston, MA 02115, USA.
Phone: (617)355-5746; Fax: (617) 730-0392; E-mail: anne.fulton@childrens.harvard.edu